An Experimental Study on Ultimate Bearing Capacity of a Foundation in Anisotropic Rock Masses

Ajay Bindlish[1]
Mahendra Singh[2*]
N. K. Samadhiya[2]

[1]*Civil Engineering Dept.*
University College of Engineering
Rajasthan Technical University
Kota – 324 010 (India)

E-mail: ajaybindlish67@rediffmail.com

[2]*Civil Engineering Dept.*
IIT Roorkee, Roorkee – 247 667 (India)

[*]*E-mail of Corresponding Author: singhfce@iitr.ernet.in*

ABSTRACT

Rock Masses encountered beneath the foundations of heavy civil engineering structures are generally jointed and anisotropic in mechanical behavior. General approach to estimate the bearing capacity of shallow foundations in such rock masses is to consider the rock mass an isotropic continuum. Very few studies are reported in literature which consider the anisotropy in bearing capacity computations. Probably, the only methodologies suggested for anisotropic rock masses are those proposed by Prakoso and Kulhaway (2004), and, Singh and Rao (2005). Singh and Rao (2005) approach was derived from the outcome of experimental studies comprising uniaxial and triaxial tests on specimens of jointed model of plaster of Paris (POP). The approach considers four fold failure mechanism namely rotation of blocks, shearing of blocks, tensile splitting of intact rocks and sliding along the existing joint. However, no experimental or field investigation is available to validate the four fold mechanism assumed by Singh and Rao (2005). In the present study, an attempt has been made to investigate the failure mechanism of jointed blocky rock mass below shallow foundations through bearing capacity tests under plane strain conditions. Plaster of Paris has been used as a model material to simulate the intact rock material. Specimens of rock mass, having various joint configurations were assembled using plaster of Paris blocks. Broadly the jointed rock mass specimens were divided into two categories. Type-A specimens comprised of a set of continuous joints orthogonal to each other. The type-B specimens used staggered joints. The orientation of joints was varied from 0^o to 90^o for both the specimen types. A footing plate was placed on the top of the mass and was loaded up to the bearing capacity failure. The results on failure modes, anisotropy in bearing capacity and settlements are presented in this paper.

Keywords*:* Bearing capacity; Jointed rock mass; Anisotropic; Discontinuities; Joints

1. INTRODUCTION

A correct understanding of failure mechanism is essential for computing bearing capacity while designing heavy structures like dams, bridge piers, tall buildings founded on rocks. The rocks are invariably intersected by discontinuities like weak planes and joints. Due to the presence of these discontinuities, the rock mass become weak and anisotropic making it more complex to analyse. The ultimate bearing capacity of shallow foundations in such rocks is not solely governed by characteristics of the homogeneous and isotropic rock material but also depends on the characteristics of the joints and bedding planes, which form the rock foundation. A foundation on rock should, therefore, be designed with much care than a foundation on soil. Traditionally, rock masses have been considered to be isotropic continuum until recently when few studies recognized the medium to be anisotropic (Prakoso and Kulhaway, 2004 and Singh and Rao, 2005). Singh and Rao (2005) explicitly recognized the importance of anisotropic behaviour of jointed rocks and suggested a methodology for computing bearing capacity of shallow foundations placed in non Hoek-Brown rock mass. The methodology has been derived from results of tests conducted on intact and jointed rocks under uniaxial and triaxial stress conditions. The methodology assumed a four fold failure mechanism and uses Bell's approach to arrive at ultimate bearing capacity of the foundation. Though the approach has been derived from extensive tests, no validation has been carried out so far either in laboratory or in field to assess the applicability of this approach. It was therefore felt essential to experimentally investigate the behavior of foundation on rock mass containing joint sets which render anisotropy to its engineering response. The objective of the study has been to investigate the failure mechanism and anisotropy in ultimate bearing capacity of jointed blocky rock mass through physical model tests.

2. HOEK-BROWN AND NON HOEK-BROWN ROCK MASSES

A rock mass is termed to be Hoek-Brown medium if it is heavily jointed and is isotropic in engineering response. A rock mass, therefore, can be treated as a Hoek-Brown material (Hoek, 2000), if (a) the block size is small in comparison to the structure being analyzed, (b) sufficient numbers of closely spaced joints are there in the rock mass (c) surface characteristics of all the joints are similar and none of the joint sets is significantly weaker than the others. Theories defined for soils may be conveniently used for determining ultimate bearing capacity in such cases.

A non Hoek-Brown medium is referred to as a natural anisotropic jointed rock mass with the foundation-width large as compared to the joint spacing, but the number of *joint sets* is not large enough to make it isotropic in strength behavior. Also the joints may not have similar surface characteristics. The conventional soil mechanics theories are not applicable in such rocks and a different approach is required. Singh and Rao (2005) approach was suggested to handle bearing capacity problems in these rocks.

3. EXPERIMENTAL PROGRAMME

Physical model tests are one of the best ways to understand the mechanism of failure of jointed rock masses. The following carefully planned experimental programme was executed to achieve the objective of the study (Bindlish, 2007):

- Design and fabrication of a bearing capacity test apparatus for testing the model specimens in plane strain conditions.

- Selection and characterization of a suitable model material which should represent the characteristics of rock.
- Preparation and testing of Type-A rock mass specimen (Fig. 1). The rock mass specimens had two orthogonal sets of intersecting joints. The joint spacing is 25mm.
- Preparation and testing of Type-B rock mass specimen (Fig. 2). The joint set-I was continuous while the joint set-II was stepped. The stepping introduces interlocking in the rock mass. The stepping s = 0.5b, where b is the width of the block.
- A 25 mm thick steel plate of size 150 mm x 150 mm was placed at the centre of the top of the specimen to apply the vertical load on the prepared specimens.
- The vertical load and resulting vertical displacement were recorded during testing of the specimen.
- The mode of failure of each specimen was also recorded.

The summary of the testing programme is shown in Fig. 3.

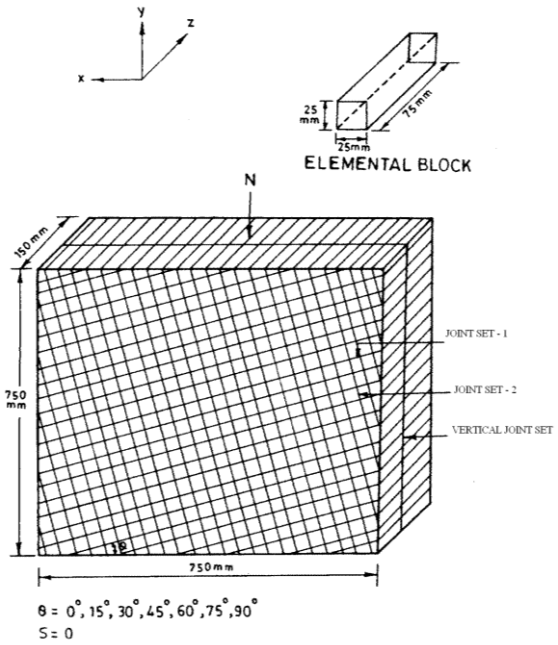

Fig. 1 - Blocky rock mass specimen having two continuous joint set (Type-A specimen, s = 0, $\theta \leq 90^o$)

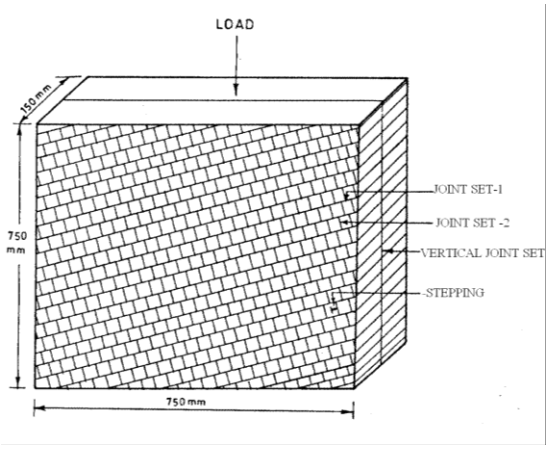

Fig. 2 - Blocky rock mass specimen having stepped joint set (Type-B specimen, s = 0.5b, $\theta \leq 90^o$)

3.1 Model Material and Its Characterization

For ease of working and reproducibility of results, model materials have been used extensively by various investigators in rock mechanics studies (Goldstein et al., 1966, Hayashi, 1966, Brown, 1970a,b, Brown and Trollop, 1970, Walker, 1971, Ladanyi and Archambault (1972), Einstein and Hirschfeld, 1973, Lama, 1974, Baoshu et al., 1986, Yang and Huang, 1995, Singh, 1997, Yang and Chiang, 2000 and Agrawal, 2005). Rock mass specimens of model material allow for better control on parameters such as intact rock strength, joint spacing, joint inclination and joint strength. A prerequisite for a study undertaken herein is that the material and joint properties should be repeatable

and controllable. The choice was therefore made to use model material rather than natural rock.

Plaster of Paris (POP) mixed with medium sand, passing through 1mm and retained on 425 micron IS sieve, was adopted as the model material for the present study. Trial specimens (diameter 38 mm and height 76 mm) were prepared by selecting different proportions of POP, sand and water. These trial specimens were air cured for 7 to 14 days and then tested in uniaxial compression. A mix proportion of 1(POP)**:** 1.25(sand)**:** 0.60(water) by weight was finally adopted, which, after 14 days of air curing was found to give the uniaxial compressive strength σ_{ci}, 7.0 MPa. The material is classified as EM as per Deere-Miller (1966) classification for intact rocks. As the UCS became nearly constant after 14 days of air curing, a curing period of 14 days was adopted.

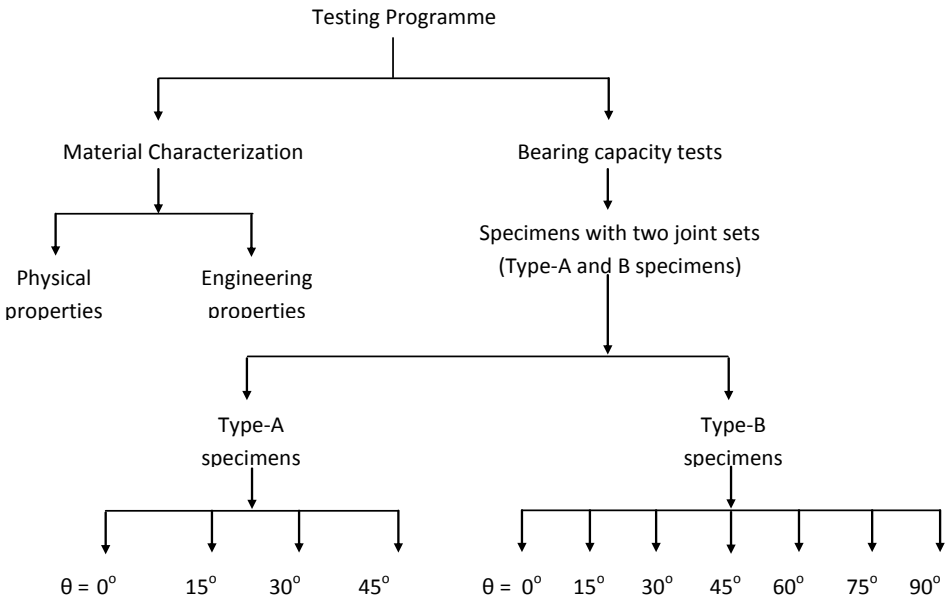

Fig. 3 - Summary of the testing programme

The physical properties of the model material were obtained as per the suggested methods of ISRM (1981). However, the uniaxial and triaxial strength tests were conducted on cylindrical cores of 38 mm diameter and 76 mm height. Triaxial tests were conducted at confining pressures equal to 0.5, 1.0, 1.5 and 2.0 MPa respectively to obtain the shear strength parameters of the intact material. The tensile strength was obtained from Brazilian tests. The cohesion c_j and friction angle of the joints, ϕ_j were obtained by conducting conventional direct shear tests along the mating surfaces of the blocks of size 6cm x 6cm x 1.5cm under low normal stress range of 50, 100, 150, 200, 250, 300, 350 and 400 kPa, respectively. The properties of the model material are presented in Table 1.

3.2 Specimen Description

3.2.1 Type-A specimens

The jointed blocky mass specimens consisted of two sets of intersecting orthogonal

joints (Fig 1). Both the joint sets were continuous. The joints in set-I were inclined at an angle θ^o with the horizontal. The angle 'θ' has been varied from 0^o to 90^o at an interval of 15^o. The joint configuration of the specimen is designated as $0^o/90^o$, $15^o/75^o$, $30^o/60^o$ and $45^o/45^o$, respectively.

Table 1 - Physical and engineering properties of the model material

Property	Value
Dry unit weight, γ_d (kN/m^3)	16.0
Specific gravity, G	2.77
Uniaxial Compressive Strength, σ_{ci} (MPa)	7.00
Failure strain, ε_f (%)	0.50
Tangent modulus, E_{t50} (MPa)	2400
Brazilian strength , σ_{ti} (MPa)	1.31
Friction angle of joint, ϕ_j (degree)	39.0
Friction angle of intact model material, ϕ_i (degree)	33.0
Cohesion of intact model material, c_i (MPa)	2.1
Deere-Miller (1966) classification	EM

3.2.2 Type-B specimens

The specimens again consisted of two sets of intersecting orthogonal joints. The joint set-I having inclination θ^o with the horizontal was continuous while joint set-II was stepped (Fig. 2). The angle 'θ' was varied from 0^o to 90^o at an interval of 15^o. The joints in the set-II were stepped at stepping 's' equal to half the width of elemental block. The joint configurations tested were $0^o/90^o$, $15^o/75^o$, $30^o/60^o$ and $45^o/45^o$, respectively.

3.3 Equipment Used

To test the blocky rock mass specimens of size 750mm x 750mm x 150mm under plane strain condition, a large size bearing capacity test apparatus was designed and fabricated in the Geotechnical Engineering Laboratory at IIT Roorkee. The apparatus consists of the following parts:

- Loading frame of 1000 kN capacity,
- Arrangement for applying plane strain conditions,
- Arrangement for applying vertical load, and
- Arrangement for measuring settlements.

3.3.1 Loading frame of 1000 kN capacity

A loading frame of 1000 kN capacity was fabricated using 20 mm thick steel plates. The frame has been designed so as to keep the plane strain apparatus in between the pillars of the loading frame. The diameter of the pillars used is 100 mm. The bottom

plate of the frame is fixed whereas the upper plate is movable to adjust the space required for placing plane strain apparatus, hydraulic jack and proving ring.

3.3.2 Arrangement for applying plane strain conditions

The plane strain box was fabricated using 10 mm thick mild steel plates on three sides while the front of the box was made from perspex sheet to allow viewing of the mechanism and failure process occurring within the specimen during testing. The Perspex sheet was properly braced by steel angles (stiffeners) so that the displacement and hence the strain in the z-direction is restricted. Similar stiffening was done on the opposite side steel plate. The rock mass specimens were assembled in the plane strain apparatus itself. The top of the box was kept open for applying the vertical load. A 25 mm thick steel test plate of size 150 x 150mm, which simulates a footing, was placed at centre of the top of the specimen.

3.3.3 Arrangement for applying vertical load

The vertical load on the test plate was applied through a hydraulic jack by taking reaction from loading frame. A proving ring was placed between the hydraulic jack and upper plate of the loading frame to measure vertical load.

3.3.4 Arrangement for measuring settlement

A steel strip was fixed between the back pillars of the loading frame with the help of the clamps. The magnetic bases of all the dial gauges were placed on this plate. To measure vertical settlements, two dial gauges were used on the opposite sides of the plate. Settlement of the footing, corresponding to a given load was taken as the average of the settlement measured by these two dial gauges. The overall view of the apparatus with specimen and loading arrangement is shown in Fig. 4.

3.4 Preparation of Blocky Mass Specimens with Two Joint Sets

The joint configurations of the blocky mass specimens, used in the present study, are already shown in Figs. 1 and 2 respectively. The blocks of model material of size 25 x 25 x 75mm were used to form the specimens. The specimens with desired joint configurations were prepared in the following manner:

3.4.1 Preparation of model material blocks

i. A dry mixture of plaster of Paris and sand in the specified proportion was prepared. Water in the required quantity was added in the dry mix and proper mixing of the material was carried out.
ii. The prepared model material mix was poured into the steel mould and of internal dimension of 250 mm length x 250 mm width x 80 mm height. The internal sides of the moulds were greased with mobil oil before pouring Plaster of Paris.
iii. The mould was shaken on vibration table for about 2 minutes to remove any entrapped air in the mix.
iv. The moulds were opened after 1 hour and were air cured for a minimum period of 14 days.

v. A large number of blocks were prepared and stacked for future use.

3.4.2 Cutting of model material blocks into elemental blocks

A specially designed and fabricated cutting arrangement was used to cut the model material blocks into elemental blocks of desired dimensions. The initial dimension of the model material blocks were 250 x 250 x 80 mm. The sides of the blocks that came in contact with oiled wall of the mould during casting were cut as wastage. The blocks were cut to form the elemental blocks in the following sequence.

i. The model material blocks were cut into slices of dimensions 250 x 80 x 25 mm each. Eight such slices were obtained from each mould .
ii. The slices obtained from step (i) were again dressed into size 240mm x 75mm x 25mm by cutting it from both sides.
iii The slices obtained from step (ii) were converted into required block size by cutting them lengthwise. The gap between the blade and the adjustable lever was adjusted to 25mm for the above purpose. Elemental blocks of size 25 x 25 x 75mm were thus obtained. A total of 64 elemental blocks were obtained from one mould.

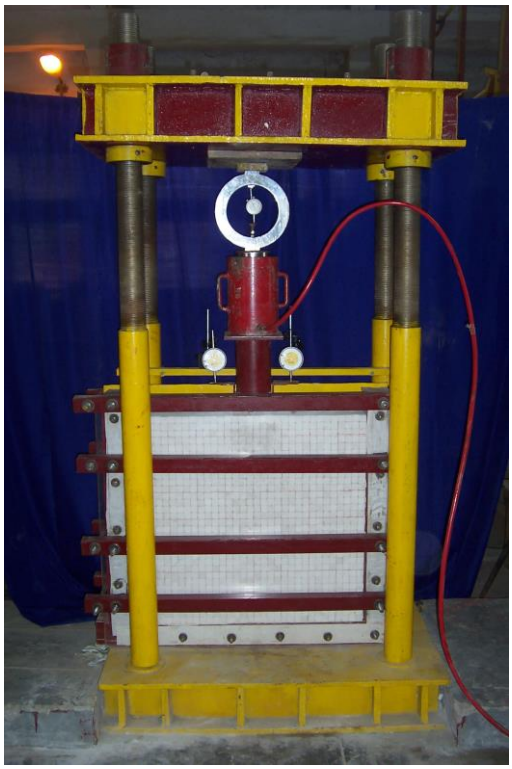

Fig. 4 - An overall view of bearing capacity test apparatus

3.4.2 Assembling of specimens

The elemental blocks of model material were assembled in a certain fashion to form the rock mass specimens. The specimens were prepared in the plane strain apparatus itself. Wooden wedges were used at the bottom and the side of rock mass specimen for creating the desired joint configuration. The wedges of specific shape and dimension were placed in the bottom of the box, and, the elemental blocks were assembled on the

wedges to form the mass. Similar wedges prepared from the model material were also placed on the top of the assembled specimen so as to obtain a finished horizontal top surface over which the test plate was placed. The clear height of the blocky mass specimen, excluding the height of bottom wedges, was 750 mm. Extreme care was taken in assembling of the elemental blocks and after a few initial trials, it was possible to prepare good quality specimens.

The specimens having stepped joints were also assembled in the similar way with the difference that an elemental block of width equal to the required stepping was placed at the bottom at the start of each alternate row or column. A brickwork type of pattern was obtained.

3.5 Testing of Specimens

The prepared specimens were tested in the large size bearing capacity test apparatus under plane strain condition. The tests were performed in the following sequence:

i. A test plate (150mm x 150mm x 25mm thick) simulating a rigid footing was placed at the centre on the top of the prepared rock mass specimen. Another steel plate of the same dimensions and having steel angles welded on both sides was kept over it to increase the thickness of the footing for allowing the large vertical displacement. A 100 mm diameter hollow MS pipe, with 10mm thick steel plates on both sides, was used above the MS footing plate as spacer. Above this spacer, a hydraulic jack of 1000 kN capacity was placed. A proving ring of 300 kN capacity was placed over the jack to measure the vertical load. The remaining gap between the proving ring and the upper plate of the loading frame was filled through spacer plates of suitable thickness.
ii. The vertical load was applied using hydraulic jack and load was measured through proving ring. The load was applied by displacing the test plate at a rate of about 1mm/minute till the specimen failed in bearing.
iii The settlement of the footing during loading was measured at two points through two dial gauges attached with the footing plate. The value of the settlement was taken as the average of the two values.
iv After each test, the dial gauges were removed from the apparatus. The upper steel plates, proving ring, hydraulic jack were then removed. The steel angles used for bracing the plane strain apparatus were then opened. The extents of damage and failure modes of the specimen were recorded.

It may be noted that the time taken from casting of model material plates to the testing of the specimen was about 36 days, however while working on mass scale in cyclic process, the average time required for one specimen could be reduced to about 21 days.

4. RESULTS AND DISCUSSIONS

4.1 Failure Mode

In the present study, ‘shear and splitting’ has been identified as the dominating failure mode beneath the footing. In the mass adjoining to the footing, loosening of the blocks associated with very slight rotation has been observed. Shear and splitting mode of failure was observed in almost all the specimens.

4.1.1 Type-A specimens (θ = 0 to 90°)

Rock mass specimens after failure are shown in Fig. 5(a-d) and details are shown in Table 2. A compressed zone has been observed at the centre from base of the footing. The boundaries of this zone are defined by joint planes. Openings of joints and relative displacements were also observed along the boundaries of the compressed zone. Maximum settlement was observed for 45°/45° and minimum was for 00°/90° case. However, the displacement of the elemental blocks below the footing were observed up to a depth of about 60cm, 55cm, 50cm, and 35cm from the top surface for the specimens having joint configuration 00°/90°, 15°/75°, 30°/60° and 45°/45° respectively.

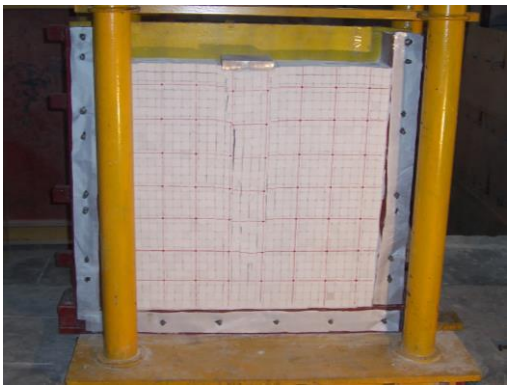

Fig. 5(a) - Failure mode in type-A specimen, 0°-90° (θ = 0°, s = 0)

Fig. 5(b) - Failure mode in type-A specimen, 15°-75° (θ =15°, s = 0)

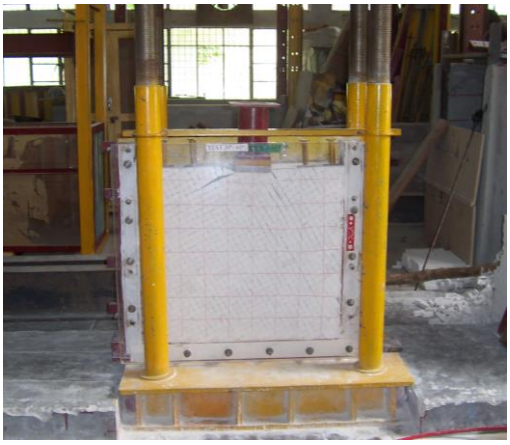

Fig. 5(c) - Failure mode in type-A specimen, 30°-60° (θ = 30°, s = 0)

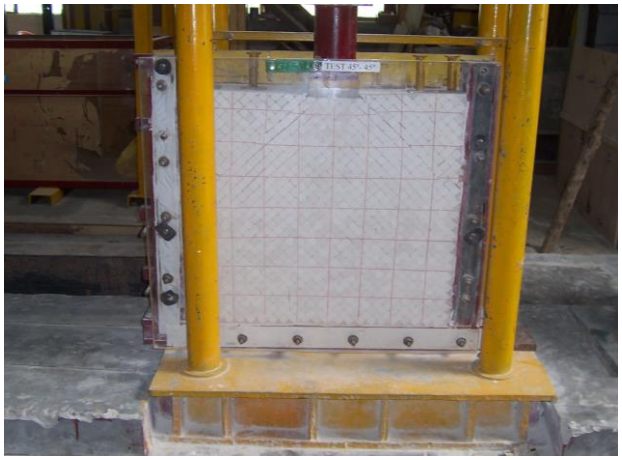

Fig. 5(d) - Failure mode in type-A specimen, 45°-45° (θ =45°, s = 0)

4.1.2 Type-B specimens (θ = 0 to 90°, s = 0.5b)

Rock mass specimens after failure are shown in Fig. 6(a-g) and details are shown in Table 3. A compressed zone was observed beneath the footing with the difference that for 90°/0° configuration, the width of the zone was equal to the plate width. With the increase in θ, the base width of this zone increased and reached its maximum value for 0°/90°. The displacement of the elemental blocks was observed up to a depth of about 30cm, 45cm, 36cm, 36cm, 36cm 56cm and 56cm from the top surface for the specimens having joint configuration 0°/90°, 15°/75°, 30°/60°, 45°/45°, 60°/30°, 75°/15°, and 90°/0° respectively.

Table 2 - Summary of experimental observations of Type-A specimens
($s = 0$, $\theta = 0^o$ to 90^o)

Joint Configuration	Experimental Observations
$00^o/90^o$	- Formation of compressed zone just below footing. This zone extends upto a depth of about 4.0 times the footing size. - Shear and splitting failure mode beneath the footing.
$15^o/75^o$	- The compressed zone below footing bounded by joint plane dipping at 75° - Shear and splitting failure mode beneath the footing. - Joint dipping at 75° on right hand side of the footing opened up to 1-2 mm. - Displacements of rock blocks observed up to a depth of 55 cm from footing base.
$30^o/60^o$	- The compressed zone below footing is bounded by joint dipping at 60° - Shear and splitting failure mode beneath the footing - The joint dipping at 30° on the left hand side of the footing and dipping at 60° on right hand side opened upto 2mm to 6mm at the time of failure. - Displacements of blocks observed up to a depth of 50 cm from footing base
$45^o/45^o$	- The compressed zone below footing is bounded by joints dipping at 45° on both sides of footing. - Shear and splitting failure mode beneath the footing. - The joint dipping at 45° on left hand side and right hand side of footing opened upto about 2 mm to 4 mm. - Displacements of the blocks observed up to a depth of about 35cm from footing base.

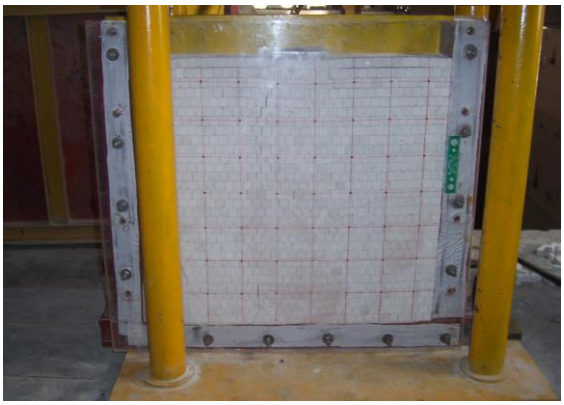

Fig. 6(a) - Failure mode in type-B specimen, 0^o-90^o ($\theta = 0^o$, $s = 0.5b$)

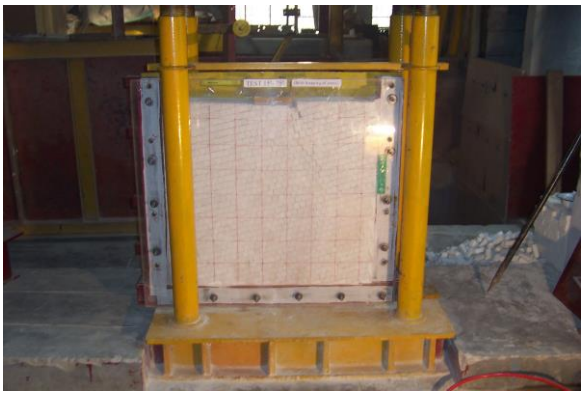

Fig. 6(b) - Failure mode in type-B specimen, 15^o-75^o ($\theta = 15^o$, $s = 0.5b$)

Fig. 6(c) - Failure mode in type-B specimen, 30º-60º (θ =30º, s = 0.5b)

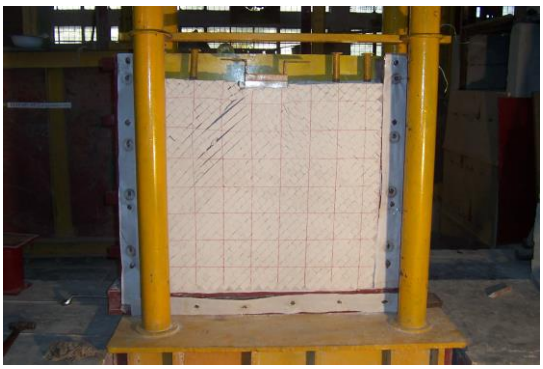

Fig 6(d) - Failure mode in type-B specimen, 45º-45º (θ =45º, s = 0.5b)

Fig 6(e) - Failure mode in type-B specimen, 60º-30º (θ =60º, s = 0.5b)

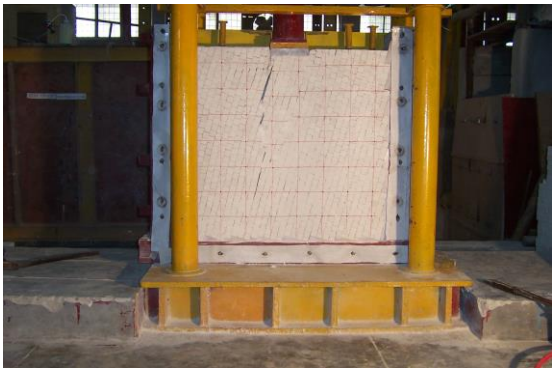

Fig. 6(f) - Failure mode in type-B specimen, 75º-15º (θ =75º, s = 0.5b)

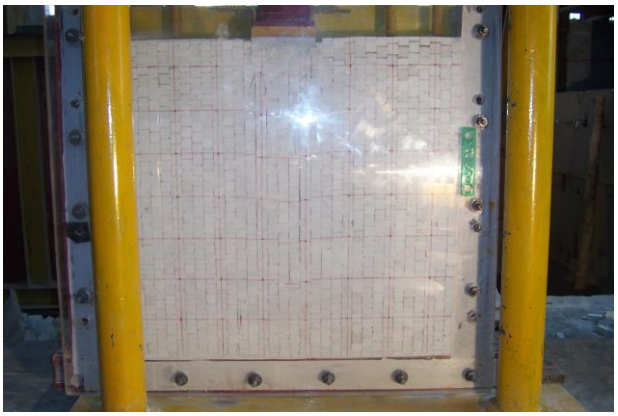

Fig. 6(g) - Failure mode in type-B specimen, 90º-0º (θ =90º, s = 0.5b)

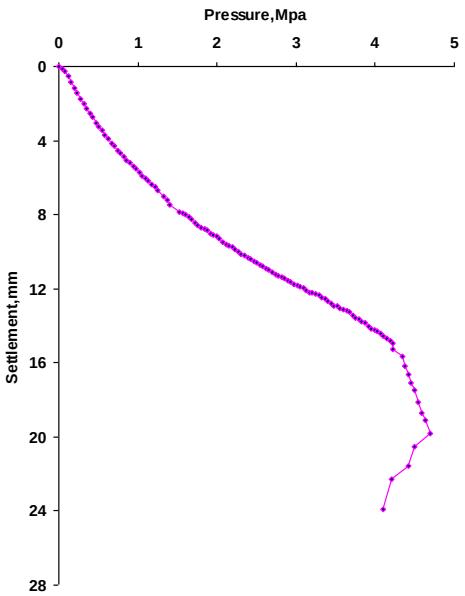

Fig. 7- Pressure vs. settlement curve for Type-A specimen, 15º-75º (θ = 15º, s = 0)

Table 3 - Summary of Experimental Observations of Type-B Specimens
($s = 0.5b$, $\theta = 0^o$ to 90^o)

Joint Configuration	Experimental Observations
$00^o/90^o$	- Formation of a compressed zone from base of footing. - Shearing and splitting failure mode beneath the footing. - Displacements observed up to a depth of 30cm from footing base
$15^o/75^o$	- Shearing of elemental blocks at the right hand side corner of the footing. - Shearing and splitting of blocks beneath the footing. - The joint dipping at 75° on the right hand side of the footing opened upto 1mm to 2mm at the time of failure. - Displacements observed up to a depth of 46 cm from footing base
$30^o/60^o$	- Shearing of the elemental blocks at the right hand side corner of the footing. - Shearing and splitting of blocks beneath the footing. - The joint dipping at 30° on the left hand side of the footing opened upto 6mm to 8mm and dipping at 60° on right hand side opened upto 1mm to 2mm at the time of failure. - Displacements observed up to a depth of 36 cm from footing base
$45^o/45^o$	- Shearing of the elemental blocks at the right hand side corner of the footing. - Shearing and splitting failure mode beneath the footing. - An opening of the joint of 5-7mm width extended from the left hand side corner of the footing and dipped at 45° and an opening of the joint of 1-1.5mm width which extended from the outer corner of the footing and dipped at 45°on the right hand side of the footing - Displacements up to a depth of 36 cm from footing base
$60^o/30^o$	- Shearing of the elemental blocks at the left hand side corner of the footing. - Shearing and splitting failure mode beneath the footing. - An opening of the joint of 3-6 mm width extended from the left hand side corner of the footing and dipped at 60° and an opening of the joint of 1mm width which extended from the outer corner of the footing and dipped at 30°on the right hand side of the footing - Displacements up to a depth of 36 cm from footing base
$75^o/15^o$	- Elemental blocks at the left hand side corner of the footing got sheared - Shearing and splitting failure mode beneath the footing. - An opening of the joint of 3-7mm width extended from the left hand side corner of the footing and dipped at 75° and an opening of the joint of 1mm width which extended from the outer corner of the footing and dipped at 15° on the right hand side of the footing - Displacements up to a depth of 56 cm from footing base
$90^o/00^o$	- A vertical compressed zone formation in the rock mass. - Shearing and splitting failure mode beneath the footing. - Displacements up to a depth of 56 cm from footing base

4.2 Pressure vs. Settlement Results

Bearing Pressure vs. settlement curves for all the specimens were obtained. One such typical curve for type-A specimens is presented in Fig. 7. The maximum value of the bearing pressure has been considered as the ultimate bearing capacity of the footing. The majority of the curves are similar in shape. The shape of the pressure vs. settlement curves is non linear with low gradient at the origin. The gradient goes on increasing with increase in settlement. The curve becomes flat as it approaches the peak. In general, there was no sudden drop in vertical stress level beyond peak which indicates progressive failure. The outcome of these plots is presented in a tabular form (Tables 4 & 5) in which the ultimate bearing capacity values and settlements observed for various joint configurations are reported.

Table 4 - Test results on ultimate bearing capacity and settlement for type-A specimens ($\theta = 0^o$ to 90^o)

Joint configuration	Ultimate bearing capacity (MPa)	Settlement of footing	
		mm	% of plate size
$00^o/90^o$ (s = 0, $\theta = 0^o$)	3.87	14.77	9.84
$15^o/75^o$ (s = 0, $\theta = 15^o$)	4.69	19.82	13.21
$30^o/60^o$(s = 0, $\theta = 30^o$)	5.18	21.31	14.20
$45^o/45^o$ (s = 0, $\theta = 45^o$)	6.25	25.57	17.04

Table 5 - Test results on ultimate bearing capacity and settlement for type-B specimens ($\theta = 0^o$ to 90^o)

Joint configuration	Ultimate bearing capacity (MPa)	Settlement	
		mm	% of plate size
$00^o/90^o$ ($\theta = 0^o$)	7.65	21.87	14.58
$15^o/75^o$ ($\theta = 15^o$)	7.14	19.66	13.10
$30^o/60^o$ ($\theta = 30^o$)	6.65	17.84	11.89
$45^o/45^o$ ($\theta = 45^o$)	6.45	17.18	11.45
$60^o/30^o$ ($\theta = 60^o$)	5.67	17.17	11.44
$75^o/15^o$ ($\theta = 75^o$)	5.18	15.29	10.19
$90^o/00^o$ ($\theta = 90^o$)	3.82	10.14	6.76

4.3 Anisotropy in Ultimate Bearing Capacity

To assess the anisotropic behavior of specimens having continuous joint sets (s = 0), the ultimate bearing capacity is plotted against joint orientation θ (Fig. 8a). For all the type-A specimens, the minimum ultimate bearing capacity is found to occur for the joint orientation $\theta = 0^o$ and $\theta = 90^o$. Ultimate bearing capacity is found to be maximum for joint orientation $\theta = 45^o$. The ratio of maximum to minimum value of ultimate bearing capacity, defined as anisotropy ratio, for type-A specimens is obtained as 1.61. The anisotropy may be classified as low anisotropic (Ramamurthy, 1993).

Anisotropy in ultimate bearing capacity of Type-B specimens may be observed from the plot given in Fig. 8b. The minimum ultimate bearing capacity has been observed to be for the joint orientation $\theta = 90^o$ whereas the maximum value is obtained for joint orientation $\theta = 0^o$. The anisotropy ratio is obtained as 2.0. The anisotropy may be classified as moderately anisotropic (Ramamurthy, 1993). The ultimate bearing capacity is found to decrease with the increase in joint orientation $\theta = 0^o$ to 90^o.

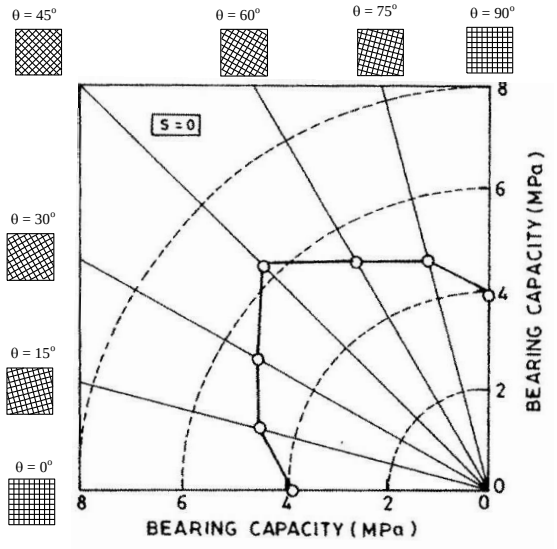

Fig. 8(a) - Graphical representation of anisotropy in ultimate bearing capacity (Type-A specimens)

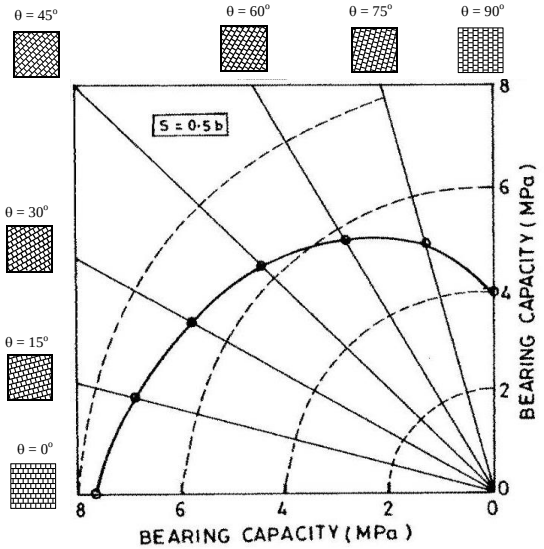

Fig. 8(b) - Graphical representation of anisotropy in ultimate bearing capacity (Type-B specimens)

It is observed that the anisotropy ratio varies from 1.61 for Type-A specimens to 2.0 for Type-B specimens. The stepping may therefore be said to have increased anisotropy in ultimate bearing capacity. This observation is quite logical as there may be enhancement in bearing capacity due to resistance offered by the stepping specially when the loading direction is normal to the stepping (Type-B, $\theta = 0°$). Due to stepping of joints, the pressure acting over the bearing area is distributed on wider area below the plate in case of $\theta = 0^o$. In case of $\theta = 90^o$ the footing applies load on a pile of block which virtually acts like a column; very little or no confinement is mobilized in this case, on the sides of loaded column. As a result, the pressure does not distribute laterally and the pressure bulb extends to great depths below the footing. Due to deeper pressure bulb, the bearing capacity may be expected to be less and settlements large. This observation has important significance in the field and suggest that in case of vertical joints, the bearing capacity may be very low and pressure bulb goes very deep, which need careful attention. Similar observations have been made by Singh (1973).

4.4 Effect of Stepping on Ultimate Bearing Capacity

The stepping, in this study, is considered to be an indirect way of introducing interlocking in the mass. In the field, termination index (ISRM, 1978) gives an idea of the interlocking of the mass. The effect of stepping on the ultimate bearing capacity of specimens with two joint set is explained in the following paragraphs:

To evaluate the effect of stepping, the ultimate bearing capacity values for the specimens with stepped joints are compared with those of continuous joints for the corresponding joint orientations. The effect of stepping on ultimate bearing capacity has been observed to be substantial for the specimens having joint orientation $\theta = 0^o$ to 45^o as shown in Fig. 9. The percent increase in ultimate bearing capacity due to stepping, over that of without stepping, was found to be 97.6%, 52.4%, 27.9% and 3.2% for the specimens having joint orientations $\theta = 0°$, 15°, 30° and 45° respectively as shown in Fig. 9.

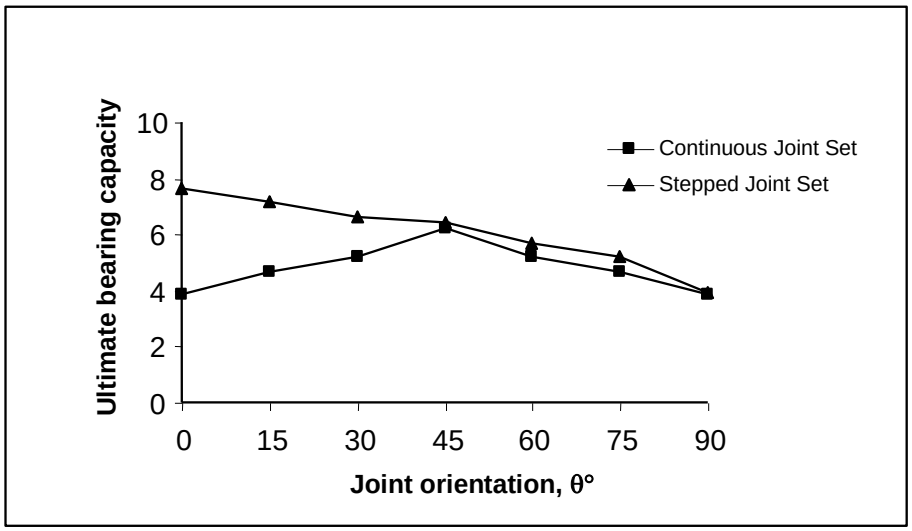

Fig. 9 - Effect of stepping on ultimate bearing capacity

The effect of stepping on ultimate bearing capacity is observed to be negligible for the specimens with joint orientation $\theta = 45°$ to 90° as shown in Fig. 9. Such a behavior is due to the fact that the continuous joints, being very steep (> 45°), facilitates movement of the mass in the dip direction of the joints and therefore there is very less interlocking effect due to stepping of the joint set-II.

5. CONCLUDING REMARKS

An experimental study has been conducted by testing rock mass specimens for bearing capacity of rock mass. Two sets of orthogonal joints have been used in the laboratory testing. The type-A specimens were prepared by adopting continuous joints whereas type-B specimens were formed by making second joint set stepped. The joint orientations were varied and tests were conducted under plain strain conditions. The results of the tests were obtained in the form of pressure vs. settlement curves for various rock mass specimens. The following conclusions are drawn from the study:

i. There is an influence zone of rock mass beneath the footing in which the mass is compressed. The zone starts from the base of the footing and is bounded by joint planes. The orientation of joints and interlocking conditions, therefore, influence the shape of the influence zone. The shape of the influence zone governs the ultimate bearing capacity and resulting settlements. A wider influence zone

indicates higher bearing capacity and low settlements whereas a narrow influence zone indicates a lower bearing capacity and higher settlements.

ii. Contrary to four fold failure mechanism, shearing and splitting has been found to be dominating failure modes of the rock mass beneath the footing. Opening of joints occurred and loose zones formed near the surface.

iii. The zone beneath the footing, in which displacement occurred, was found to be varying from 35cm (about 2.3 times the footing width, B) to 60cm (4.0 times the footing width, B) from the base of footing. The depth of this zone for type-A specimens has been found to be minimum for joint configuration 45°-45^o and maximum for 0^o-90^o, respectively.

iv. The displacements in the rock mass for type-B specimens were observed up to depth ranging from 30cm (2.0B) to 56cm (3.7B) from base of the footing. The depth of this zone has been found to be minimum for joint configuration 0^o-90° and maximum for 90^o-0^o respectively.

v. The pressure-settlement curves are found to be non linear. The gradient goes on increasing with increase in settlement. The curve becomes flat as it approaches the peak. In general, there was no sudden drop in vertical stress level beyond peak stress indicating progressive failure.

vi. The ultimate bearing capacity has been found to be anisotropic in nature. For type-A specimens, the anisotropy ratio is 1.61. Ultimate bearing capacity is found to be maximum for the specimen with joint configuration 45^o-45^o and minimum for joint configuration 0^o-90^o, respectively. Vertical joints represent the most unfavorable joint condition for both specimen types.

vii. For type-B specimens, the anisotropy ratio is 2.0. The minimum ultimate bearing capacity occurs for the specimen with joint configuration is 90^o- 0^o and maximum with joint configuration 0^o-90^o.

viii. The stepping in this study is an indirect measure of interlocking conditions and has been found to have substantial effect on ultimate bearing capacity for joint orientation $\theta = 0^o$ to 45^o. The percent increase in ultimate bearing capacity due to stepping, over that of without stepping, was found to be 97.6%, 52.4% and 27.9% for the specimens having joint orientations $\theta = 0°$, 15° and 30° respectively. However, the stepping is found to have negligible increase in ultimate bearing capacity in the range of $45° \leq \theta \leq 90°$. The reason being the shape of compressed zone. In case $\theta \leq 45°$, the zone is wide due to stepping, for $\theta \geq 45°$, the loading direction coincides with joint dip and compressed zone is limited to foundation width and the dispersion of stress does not occur.

Acknowledgement

The work presented in this paper has been a part of the Ph. D. thesis of the first author which was completed under the supervision of co-authors at I. I. T. Roorkee under Quality Improment Programme of Government of India. The first author is thankful to the authorities at University College of Engineering, Rajasthan Technical University, Kota for sponsoring him for Ph. D. The authors are also thankful to Prof. Bhawani Singh and Prof. M. N. Viladkar for their valuable guidance during the Ph. D. programme.

Notations:

B	Width of the footing
b	Width of block = 25mm
c_i and ϕ_i	Shear strength parameters of intact rock
q_{ult}	Ultimate bearing capacity
r	Joint strength parameter
s	Stepping of joint
β	Orientation of joint plane w.r.t. loading direction
γ	Unit weight of the rock mass
γ_d	Dry density
ϕ	Friction angle
ϕ_j	Joint friction angle
θ	Dip of joint plane w. r. t. horizontal
σ_n	Applied normal stress
σ_{cj}	UCS of jointed rock; Apparent rock mass strength
σ_{ci}	Uniaxial compressive strength of the intact rock

References

Agarwal, B. K. (2005). *Shear Strength Behaviour of Jointed Model Material Under Low CNL Condition*, Ph.D. Thesis, IIT Roorkee, Roorkee, India.

Baoshu, G., Huoyao, X. and Hanmin, W. (1986). An Experimental Study on the Strength of Jointed Rock Mass, *Proc. of Int. Symp. on Engineering in Complex Rock Formations*, 3-7 Nov, Beijing, China, pp.190-198.

Bindlish, A. (2007). *Bearing Capacity of Strip Footings on Jointed Rocks*. Ph.D. Thesis, Civil Engg. Deptt., I. I.T., Roorkee, India.

Brown E.T. and Trollope D.H. (1970). Strength of a Model of Jointed Rock, *J. of Soil Mech. & Found. Div., Proc. ASCE*, 96(SM2), 685-704.

Brown E.T. (1970a). Strength of Models of Rock with Intermittent Joints, *J. of Soil Mech. & Found. Div., Proc. ASCE*, 96(SM6), pp.1935-1949.

Deere, D.U., Miller, R.P. (1966). Engineering Classification and Index Properties for Intact Rock, *Technical Report No. AFNL-TR-65-116.* Air Force Weapons Laboratory, New Mexico.

Einstein, H.H. and Hirschfeld, R.C. (1973). Model Studies on Mechanics of Jointed Rock, *J. of Soil Mech. & Found. Div. Proc. ASCE*, 90, pp. 229-248.

Goldstein, M., Goosev, B., Pyrogovsky, N., Tulinov, R. and Turovskaya, A. (1966). Investigation of Mechanical Properties of Cracked Rock, *Proc. Ist Cong. ISRM*, Lisbon, 1, 521-524.

Hatashi, M. (1966). Strength and Dialatancy of Brittle Jointed Mass - The Extreme Value Stochastic and Anisotropic Failure Mechanism., *Proc Ist Cong. ISRM*, Lisbon, 1, pp.295-302.

Hoek, E. (2000). Practical Rock Engineering, 2000 Edition, http://www.rocscience.com/hoek/Practical RockEngineering.asp.

ISRM (1981). *Rock Characterization, Testing and Monitoring*. ISRM Suggested Methods. Brown E.T. (*ed*.), Pergamon Press.

Ladanyi, B. and Archambault, G. (1972). Evaluation of Shear Strength of a Jointed Rock Mass, *Proc. 24th Int. Geological Congress*, Montreal, Section 13D, pp.249-270.

Lama R. D. (1974). The Uniaxial Compressive Strength of Jointed Rock, Prof. L. Müller Festschrift, *Inst. Soil Mech. & Rock Mech.*, Univ. Karlsruhe, Karlsruhe, pp.67-77.

Prakoso, W. A. and Kulhawy, F. H. (2004). Bearing Capacity of Strip Footings on Jointed Rock Masses, *J. of Geotechnical and Geoenvironmental Engineering*, Vol. 130(12), pp. 1347-1349.

Ramamurthy, T. (1993). Strength and Modulus Response of Anisotropic Rocks, Chapter 13, *Comprehensive Rock Engg*., Vol 1, Pergamon Press, U.K., pp. 313-329.

Singh, B. (1973). Continuum Characterization of Jointed Rock Mass Part II – Significance of Low Shear Modulus, *Int. J. Rock Mech. And Min. Sci. & Geomech. Abstr*., Pergamon, Vol. 10, pp. 337-349.

Singh, M. (1997). *Engineering Behaviour of Jointed Model Materials*, Ph.D. Thesis, IIT Delhi, India.

Singh, M. and Rao, K. S. (2005). Bearing Capacity of Shallow Foundations in Anisotropic Non Hoek-Brown Rock Masses, *J. of Geotechnical and Geoenvironmental Engineering*, Vol. 131(8), pp. 1014-1023.

Sutcliffe, D. J., Yu, H. S. and Sloan, S.W. (2004). Lower Bound Solutions for Bearing Capacity of Jointed Rock, *Computers and Geotechnics*, Vol. 31(1), pp. 23-36.

Walker, P. F. (1971). *The Shearing Behaviour of Block Jointed Rock Model*, Ph.D. Thesis, Queens Univ., Belfast

Yang, Z. Y., Huang, T. H., (1995). Effect of Joint Sets on the Anisotropic Strength of Rock Masses, *Proc. 8th Cong. ISRM*, Japan, pp.367-370.

Yang, Z. Y. and Chiang, D.Y. (2000). An Experimental Study on the Progressive Shear Behaviour of Rock Joints with Tooth-Shaped Asperities, *Int. J. of Rock Mechanics and Mining Science*s, 37, pp.1247-1259.